applied sciences

MDPI

Article

Generating Radially and Azimuthally Polarized Beams by Using a Pair of Lateral Displacement Beamsplitters

Chien-Yuan Han [1], Zhi-Hao Wei [2], Yung Hsu [3], Kun-Huang Chen [4], Chien-Hung Yeh [2], Wei-Xuan Wu [2] and Jing-Heng Chen [2,*]

1 Department of Electro-Optical Engineering, National United University, No. 2, Lienda, Nanshi Li, Miaoli 36063, Taiwan; cyhan@nuu.edu.tw
2 Department of Photonics, Feng Chia University, No. 100, Wenhwa Rd., Seatwen, Taichung 40724, Taiwan; zack8006511@gmail.com (Z.-H.W.); yehch@fcu.edu.tw (C.-H.Y.); liquid9527@gmail.com (W.-X.W.)
3 Institute of Electro-Optical Engineering, National Chiao Tung University, No. 1001, University Rd., Hsinchu 30010, Taiwan; matrtihewl0937@gmail.com
4 Department of Electrical Engineering, Feng Chia University, No. 100, Wenhwa Rd., Seatwen, Taichung 40724, Taiwan; chenkh@fcu.edu.tw
* Correspondence: jhchen@fcu.edu.tw; Tel.: +886-4-2451-7250 (ext. 5093); Fax: +886-4-2451-0182

Academic Editors: Malte C. Kaluza and Shoou-Jinn Chang
Received: 27 May 2016; Accepted: 23 August 2016; Published: 27 August 2016

Abstract: This paper proposes a modified polarization converter for generating radially and azimuthally polarized beams. Based on a Mach–Zehnder-like interferometric structure, the device consists of a pair of lateral displacement beamsplitters (LDBs) and two half-wave plates that manipulate the states of polarization of incident linearly polarized light. Through the coherent superposition of two orthogonal Hermite–Gaussian modes in the far field, radially and azimuthally polarized beams can be obtained simultaneously. A prototype was assembled to demonstrate the feasibility of the design. The proposed design has the advantage of having a simple, symmetric, compact, and robust structure. In addition, the introduction of LDBs substantially reduces the cost of this device. Moreover, the design can be applied to a broadband pulsed laser with considerable potential in high-power applications.

Keywords: beam splitters; waveplates; coherence; interference; polarizations

1. Introduction

Radially and azimuthally polarized beams have been increasingly studied in recent years because of their unique characteristic of axial polarization symmetry, and they can break the diffraction limit with a strong longitudinal electromagnetic field in focus [1–3]. The applications of these beams include high-resolution microscopy, surface plasmon excitation, optical trapping, material processing, and high-density data storage [4–6]. Various generation theories and methods for these beams have been proposed. The generation methods can be categorized as intracavity and extracavity methods. For the intracavity method, a specially designed birefringent crystal, an adjustable aperture, conical and axicon prisms, or a non-periodic sub-wavelength grating is set inside the resonant cavity of a laser to generate the radially or azimuthally polarized beam [7,8]. However, laser cavity structures are typically complicated. This complicated structuring could cause difficulty for alignment and thus additional power loss in laser manufacturing. Additionally, limited by the form of the laser cavity, the intracavity method is not suitable for fiber lasers, lithography ultraviolet (UV) lasers, or semiconductor lasers. By contrast, the extracavity method (which refers to two types of techniques), achieves radially and azimuthally polarized beams outside of the laser cavity. The first type of technique uses a cut half-wave

plate, polarization converter, or liquid-crystal spatial light modulator to convert a linearly or circularly polarized beam into a radially or azimuthally polarized beam [9,10]. The second type of technique uses various interferometric structures to obtain a radially or azimuthally polarized beam [11,12]. The implementation of these methods could be restricted by the requirements of a highly coherent light source and environmental stability. This possibility makes the implementation of these methods potentially difficult. In addition, the generated beam is typically limited by low power. Phua and Lai proposed a simple manipulation method that uses birefringent crystals and half-wave plates to coherently generate a radially polarized beam [13]. In their method, the structure fulfills the demands of compactness, mechanical stability, and robustness for practical high power applications. However, because of the birefringence of the crystal polarization mode, dispersion occurs during the manipulation of different states of polarization. To eliminate the temporal walk-off problem, a second birefringent crystal is required to compensate the optical path difference between two orthogonal polarized modes. Therefore, the cost of the method could be high.

In this paper, we propose a modified method for the generation of radially and azimuthally polarized beams. Based on a Mach–Zehnder-like interferometric arrangement, a pair of lateral displacement beamsplitters (LDBs) is used to replace the expensive birefringent crystals. Half-size and full-size half-wave plates (h-HWP and f-HWP) are applied to manipulate the states of polarization of the incident beam. The operation principles of this method, accompanied with a Jones matrix calculus, are described. With coherent superposition, radially and azimuthally polarized beams can be simultaneously achieved in the far-field region. To demonstrate the feasibility of the method, a prototype of the proposed polarization converter was successfully assembled and tested. Because of the application of LDBs, the design has a simple, symmetric, compact, and robust structure; furthermore, this design reduces the cost of the device substantially. In addition, the device can operate with a broadband pulsed laser and has considerable potential for high-power applications.

2. Principles

Figure 1 illustrates the design of the optical structure for the generation of radially and azimuthally polarized beams. It consists of a pair of confocal cylindrical lenses with a focal length ratio of 1:2, a lateral displacement polarizing beamsplitter (LDPB), h-HWP and f-HWP, and an LDB. To facilitate an understanding of the principle, an orthogonal *x*-*y*-*z* coordinate system is introduced. The cross-section of the laser beam (viewing against the direction of light propagation) and the associated states of polarization after passing through each component are depicted in the four quadrants of Q_1, Q_2, Q_3, and Q_4, as shown in Figure 1a–g.

In Figure 1, the Jones column matrix for a linearly polarized beam propagating in the +*z*-direction can be expressed as [14]:

$$E(\theta) = \begin{bmatrix} \cos\theta \\ \sin\theta \end{bmatrix} \quad (1)$$

where θ indicates the direction of polarization with respect to the *x*-axis; and cosθ and sinθ represent the horizontal and vertical components of the polarization, respectively. In Figure 1a, a circular Gaussian beam with a 45° linear polarization (with respect to the *x*-axis) is incident into a pair of cylindrical lenses in the +*z*-direction. Consequently, its beam cross-section is transformed into an elliptical Gaussian beam, as illustrated in Figure 1b. After passing through the LDPB, the 45° linearly polarized elliptical Gaussian beam is separated into two orthogonally polarized components, as illustrated in Figure 1c. These components continue to pass through the h-HWP and the f-HWP. The optical axes of the h-HWP and f-HWP are set at 45° and 22.5° with respect to the *x*-axis, respectively. Therefore, as shown in Figure 1d, the states of polarization in the right-half regions (quadrants Q_1 and Q_4) for these elliptical beams are rotated by 90°. In Figure 1e, the states of polarizations at the four quadrants of these elliptical

beams are rotated by 45°. Accordingly, the Jones column vector $\boldsymbol{E_{Qi}}$ of each polarized beam at the i-th quadrant (i = 1 to 4) can be expressed as:

$$\boldsymbol{E_{Qi}} = \boldsymbol{J}_{f-HWP}(\Theta)\boldsymbol{J}_{h-HWP}(\Theta)E(\theta),\ (\text{for } i = 1 \text{ then } \theta = 0^\circ;\ \text{for } i = 4 \text{ then } \theta = 270^\circ) \quad (2)$$

and

$$\boldsymbol{E_{Qi}} = \boldsymbol{J}_{f-HWP}(\Theta)E(\theta),\ (\text{for } i = 2 \text{ then } \theta = 180^\circ;\ \text{for } i = 3 \text{ then } \theta = 90^\circ) \quad (3)$$

where $\boldsymbol{J}$ represents the Jones matrix of the half-wave plate, and Θ represents the direction of the optical axis of the half-wave plate with respect to the x-axis. Consequently, the Jones column vectors of the polarized beams at the four quadrants can be written as

$$\boldsymbol{E_{Q1}} = \begin{bmatrix} 1 \\ 1 \end{bmatrix},\ \boldsymbol{E_{Q2}} = \begin{bmatrix} -1 \\ 1 \end{bmatrix},\ \boldsymbol{E_{Q3}} = \begin{bmatrix} -1 \\ -1 \end{bmatrix},\ \text{and}\ \boldsymbol{E_{Q4}} = \begin{bmatrix} 1 \\ -1 \end{bmatrix}$$

Finally, the two polarized beams are concentrated after passing through and reflecting off the LDB, respectively. In Figure 1f,g, the beams are two sets of 45° frame-rotated Hermite–Gaussian TEM_{10} and TEM_{01} modes. Based on the image inversion caused by a right-angle prism and the reflection of polarized light, the Jones column vectors of the polarized beam (illustrated in Figure 1g) with a new set of quadrants Q_1*, Q_2*, Q_3*, and Q_4*, can be written as

$$\boldsymbol{E_{Q1}}* = \begin{bmatrix} -1 \\ 1 \end{bmatrix},\ \boldsymbol{E_{Q2}}* = \begin{bmatrix} 1 \\ 1 \end{bmatrix},\ \boldsymbol{E_{Q3}}* = \begin{bmatrix} 1 \\ -1 \end{bmatrix},\ \text{and}\ \boldsymbol{E_{Q4}}* = \begin{bmatrix} -1 \\ -1 \end{bmatrix},$$

where the direction of polarization occurs with respect to the $-z$-axis. Accordingly, approximately radially and azimuthally polarized beams can be obtained in the far field with coherent superposition [15] by using a positive imaging lens (IL). In Figure 1, the radially and azimuthally polarized beams are checked with an analyzer (AN) and a charge-coupled device (CCD) camera.

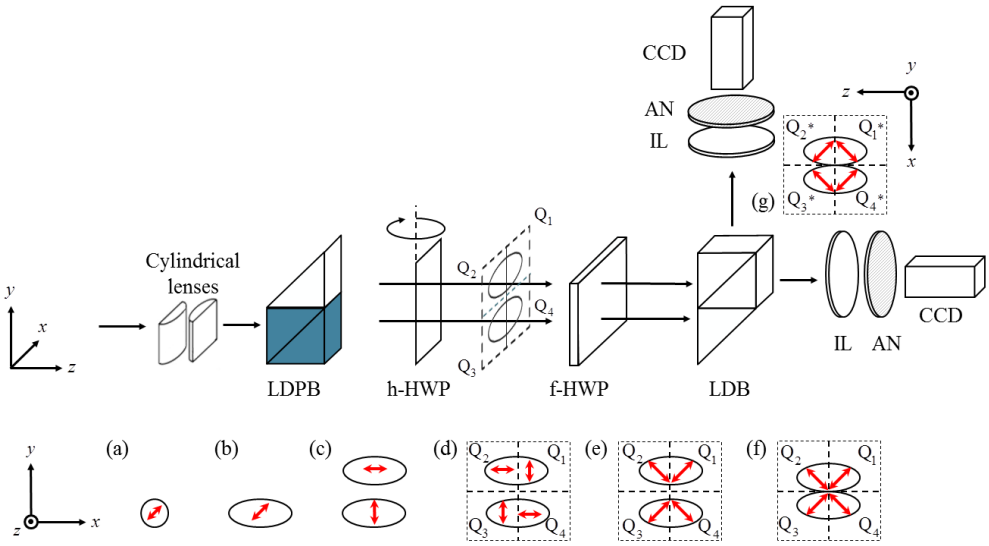

Figure 1. Schematic representation of the generation of radially and azimuthally polarized beams. The diagrams illustrate the cross-section of the laser beam and the associated states of polarizations caused by passing through (**a**) the laser; (**b**) a pair of cylindrical lenses; (**c**) the lateral displacement polarizing beamsplitter (LDPB); (**d**) the half-size half-wave plate (h-HWP); (**e**) the full-size half-wave plate (f-HWP); (**f**) the lateral displacement beamsplitter (LDB); and by reflecting off (**g**) the LDB. The coherent superposition of orthogonal polarizations in the far field is achieved with a positive imaging lens (IL) and the beam profiles are checked using an analyzer (AN) and a charge-coupled device (CCD) camera.

3. Results and Discussion

To show the feasibility of the design, a prototype of the proposed polarization converter was assembled that incorporated a pair of confocal cylindrical lenses (LJ1878L1-A; LJ1960L1-A, THORLABS) with focal lengths of 10 mm and 20 mm, respectively, a pair of lateral displacement (polarizing and nonpolarizing) beamsplitters (PBS251; BS013; PS911, THORLABS), and two multiorder half-wave plates (MOWP-633-1/2-10, BVO). The dimensions of the device were 125 × 50.8 × 25.4 mm. A 632.8 nm helium-neon laser (AH100M, ONSET) was used as the light source, with an output power of 10 mW. The phase condition between each quadrant was maintained as in-phase through angle adjustments of the h-HWP on the *y*-axis. A positive IL with a focal length of 100 mm was used to generate the radially and azimuthally polarized beams in the far field. The donut-shaped patterns are shown in Figures 2 and 3. The size of the beams illustrated in Figures 2a and 3a was approximately 200 μm. To verify the radial and azimuthal characteristic of these beams, an analyzer was applied with different azimuthal angles prior to the CCD camera (XCD-U100CR, SONY) and a laser beam profiler (BP109-VIS, THORLABS). In Figure 2b–e, the beam profiles were observed with the transmitting axis of the analyzer being 0°, 45°, 90°, and 135° with respect to the *x*-axis. In Figure 3b–e, the beam profiles were observed with the transmitting axis of the analyzer being 0°, 45°, 90°, and 135° with respect to the $-z$-axis. To examine the polarization quality of these beams, an additional quarter-wave plate (WPQ05M-633, THORLABS) was inserted prior to the analyzer for the demonstration of the spatial distributions of Stokes parameters [14,16], as shown in Figure 4. The Stokes parameter S_0 describes the total intensity of the optical beam, which was scaled between 0 and 2. The parameter S_1 is the intensity difference between horizontal and vertical polarization. The parameter S_2 represents the intensity difference between linear polarization oriented at 45° and 135°. Therefore, the values of S_1 and S_2 were between +1 and −1. The parameter S_3 describes the intensity difference between right and left circular polarization, which was scaled between +0.5 and −0.5. Ideally, the values of S_3 should be much smaller than S_0, S_1, and S_2. Although the intensity distributions did not show a good cylindrical symmetry, they could be improved by applying highly accurate translation and rotation stages for alignment. These results successfully demonstrated the feasibility of the proposed design.

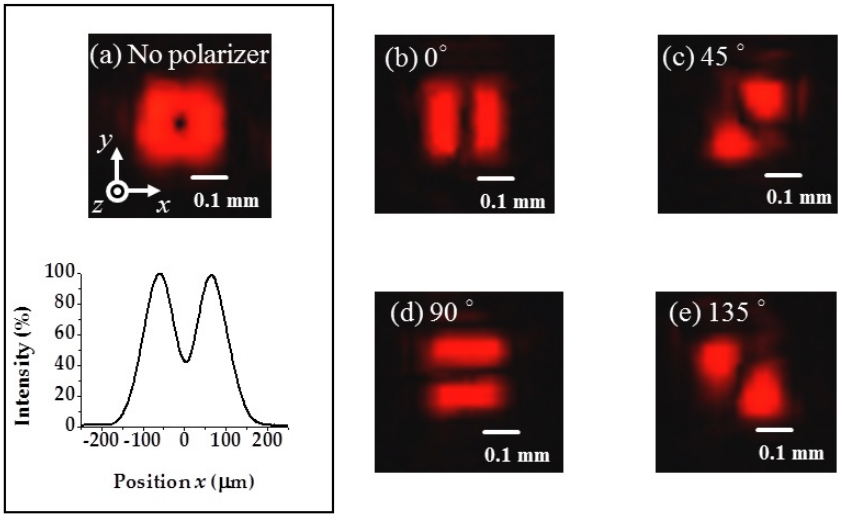

Figure 2. Radially polarized lights in the transmission output converted from a linearly polarized light: (**a**) donut-shaped beam profile and intensity distribution in the *x*-direction observed without an analyzer, and beam profiles observed with the transmitting axis of an analyzer at (**b**) 0°; (**c**) 45°; (**d**) 90°; and (**e**) 135° with respect to the *x*-axis.

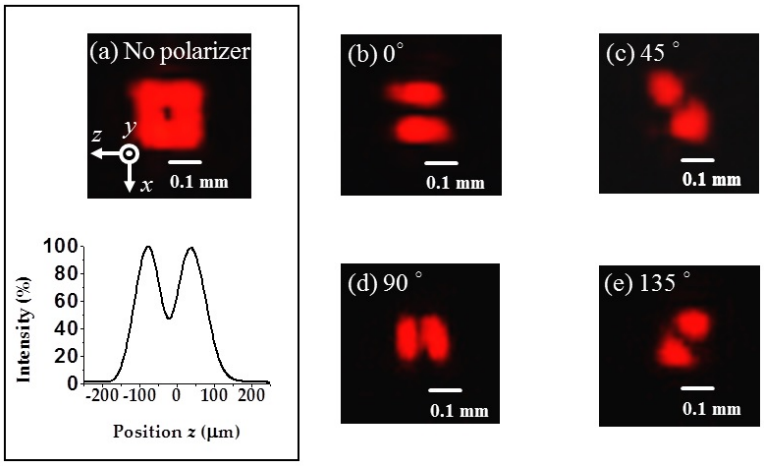

Figure 3. Azimuthally polarized lights in the reflection output converted from a linearly polarized light: (**a**) donut-shaped beam profile and intensity distribution in the z-direction observed without an analyzer, and beam profiles observed with the transmitting axis of an analyzer at (**b**) 0°; (**c**) 45°; (**d**) 90°; and (**e**) 135° with respect to the $-z$-axis.

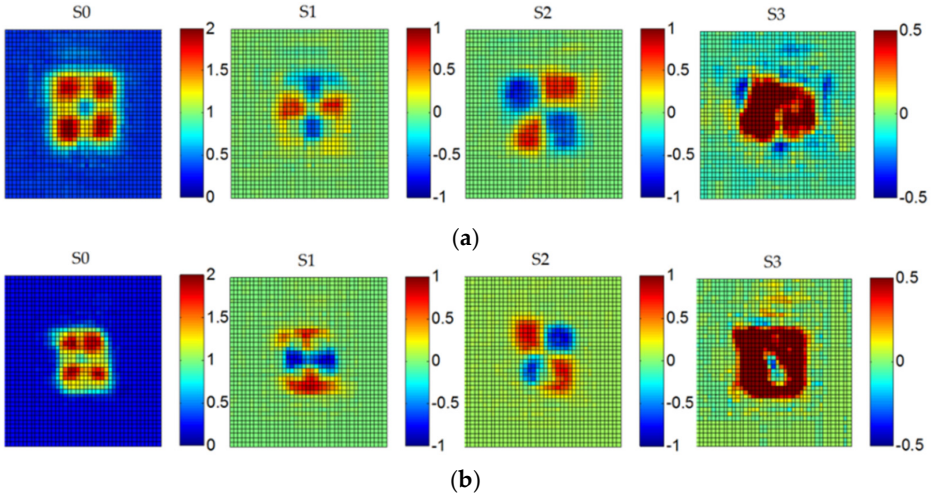

Figure 4. Spatial distributions of Stokes vectors of S_0, S_1, S_2, and S_3: (**a**) radially polarized light and (**b**) azimuthally polarized light.

The proposed polarization converter has a simple and symmetric structure that facilitates the maintenance of the in-phase condition for the generation of radially and azimuthally polarized beams. In addition, the device can generate radially and azimuthally polarized beams simultaneously. In an application, a linear superposition of radially polarized mode and azimuthally polarized mode generates cylindrical vector (CV) beams [3], as shown in Figure 5. Because two beams are always produced simultaneously, it causes 50% losses if only one beam mode is needed. In this condition, an additional reflection prism (RP) could be applied to transform one mode into another. In Figure 6a, a reflection prism is set next to the LDB, which transforms the azimuthally polarized mode into a radially polarized mode by reflection. In Figure 6b, a reflection prism is set after the LDB, which transforms the radially polarized mode into an azimuthally polarized mode by reflection. Therefore, two outputs of radially polarized beam in $+x$-direction and two outputs of azimuthally polarized beam in $+y$-direction could be achieved. A continuous wave laser was used in the experiment for demonstration. Because of the symmetric structure, the two orthogonally polarized modes have the same optical path length (OPL). Having the same OPL implies that ideally, no temporal walk-off problem exists (polarization mode dispersion) between the orthogonally polarized modes in the design.

Accordingly, the device can operate with a broadband pulsed laser. In [13], an additional crystal-type spatial walk-off polarizer was required to compensate for the OPL difference between two orthogonal polarized modes. By contrast, the cost of the proposed device can be substantially reduced by applying the lateral displacement beamsplitters. However, lateral displacement beamsplitters are commonly constructed out of a cube and a prism. These separate components could slightly complicate the device. Figure 7 illustrates that a proper shift should occur between the cube and the prism of the LDB to concentrate the polarized beams at four quadrants from a long distance L to a short distance l. When smaller components are used and glued together, a more compact and robust device can be achieved. Because of the application of bulk solid materials, the device has a high damage threshold of at least 50 W/cm^2. With the same principle, the device can be designed at an operation wavelength of 1064 nm. For high-power applications, zero-order half-wave plates should be used to eliminate the influence of the thermal effect.

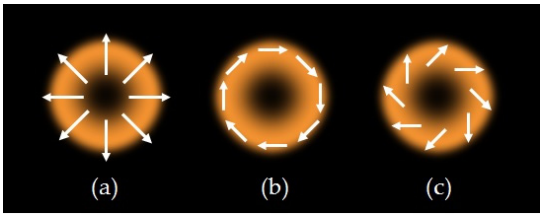

Figure 5. Spatial distributions of instantaneous electric vector field for (**a**) radially polarized mode; (**b**) azimuthally polarized mode; and (**c**) generalized cylindrical vector (CV) beams as a linear superposition of (**a**) and (**b**).

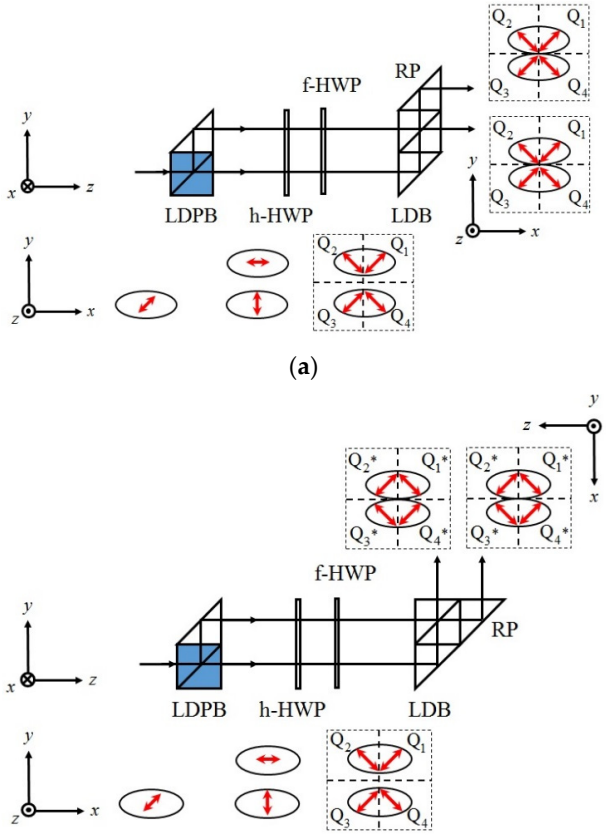

Figure 6. A reflection prism (RP) is applied to transform one mode into another: (**a**) two output radially polarized beams in the +x-direction, and (**b**) two output azimuthally polarized beams +y-direction.

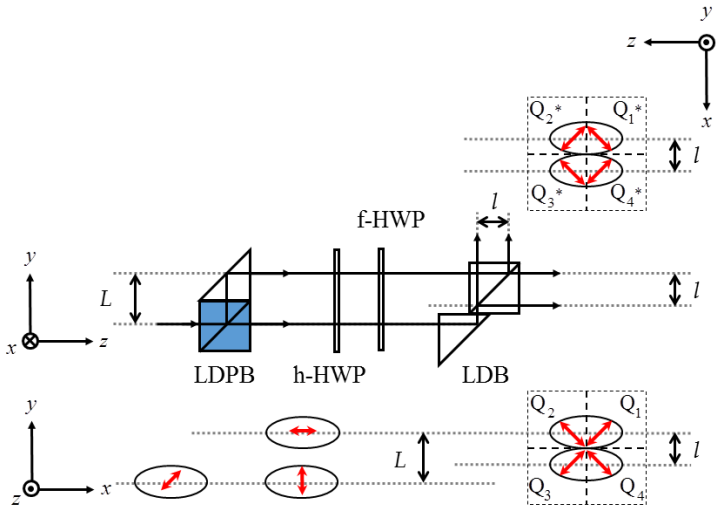

Figure 7. Lateral view of the alignment and assembly considerations of the design (not to scale).

4. Conclusions

This paper proposed an improved design for a polarization converter that can generate radially and azimuthally polarized beams simultaneously. The device applies a pair of lateral displacement beamsplitters to replace expensive crystal-type spatial walk-off polarizers. Two half-wave plates are incorporated to manipulate the states of polarization of the incident light. The design enables approximately radially and azimuthally polarized beams to be obtained in the far field with coherent superposition. A prototype of the polarization converter was successfully demonstrated, and several of its advantages were discussed. The proposed device has considerable potential for high-power applications.

Acknowledgments: This work was supported by the Ministry of Science and Technology of the Republic of China under the grant numbers MOST 104-2221-E-035-064 and MOST 105-2221-E-035-045.

Author Contributions: Jing-Heng Chen and Chien-Yuan Han conceived and designed the experiments; Zhi-Hao Wei, Yung Hsu and Wei-Xuan Wu performed the experiments; Jing-Heng Chen and Chien-Yuan Han analyzed the data; Jing-Heng Chen, Chien-Yuan Han, Kun-Huang Chen and Chien-Hung Yeh contributed the materials; and Jing-Heng Chen and Zhi-Hao Wei wrote the paper.

Conflicts of Interest: The authors declare no conflict of interest.

References

1. Dorn, R.; Quabis, S.; Lcuchs, G. Sharper focus for a radially polarized light beam. *Phys. Rev. Lett.* **2003**, *91*. [CrossRef] [PubMed]
2. Passilly, N.; de Saint Denis, R.; Aït-Ameur, K.; Treussart, F.; Hierle, R.; Roch, J.F. Simple interferometric technique for generation of a radially polarized light beam. *J. Opt. Soc. Am. A* **2005**, *22*, 984–991. [CrossRef]
3. Zhan, Q. Cylindrical vector beams: From mathematical concepts to applications. *Adv. Opt. Photonics* **2009**, *1*, 1–57. [CrossRef]
4. Niziev, V.G.; Nesterov, A.V. Influence of beam polarization on laser cutting efficiency. *J. Phys. D Appl. Phys.* **1999**, *32*, 1455–1461. [CrossRef]
5. Peng, F.; Yao, B.; Yan, S.; Zhao, W.; Lei, M. Trapping of low-refractive-index particles with azimuthally polarized beam. *J. Opt. Soc. Am. B* **2009**, *26*, 2242–2247. [CrossRef]
6. Zhang, Y.; Bai, J. Improving the recording ability of a near-field optical storage system by higher-order radially polarized beams. *Opt. Express* **2009**, *17*, 3698–3706. [CrossRef] [PubMed]
7. Li, J.L.; Ueda, K.I.; Musha, M.; Shirakawa, A.; Zhong, L.X. Generation of radially polarized mode in Yb fiber laser by using a dual conical prism. *Opt. Lett.* **2006**, *31*, 2969–2971. [CrossRef] [PubMed]
8. Bomzon, Z.; Kleiner, V.; Hasman, E. Formation of radially and azimuthally polarized light using space-variant subwavelength metal stripe gratings. *Appl. Phys. Lett.* **2001**, *79*, 1587–1589. [CrossRef]

9. Machavariani, G.; Lumer, Y.; Moshe, I.; Meir, A.; Jackel, S. Efficient extracavity generation of radially and azimuthally polarized beams. *Opt. Lett.* **2007**, *32*, 1468–1470. [CrossRef] [PubMed]
10. Bashkansky, M.; Park, D.; Fatemi, F.K. Azimuthally and radially polarized light with a nematic SLM. *Opt. Express* **2010**, *18*, 212–217. [CrossRef] [PubMed]
11. Radwell, N.; Hawley, R.D.; Götte, J.B.; Franke-Arnold, S. Achromatic vector vortex beams from a glass cone. *Nat. Commun.* **2016**, *7*, 1–6. [CrossRef] [PubMed]
12. Han, C.-Y.; Chang, R.-S.; Chen, H.-F. Solid-state interferometry of a pentaprism for generating cylindrical vector beam. *Opt. Rev.* **2013**, *20*, 189–192. [CrossRef]
13. Phua, P.B.; Lai, W.J. Simple coherent polarization manipulation scheme for generating high power radially polarized beam. *Opt. Express* **2007**, *15*, 14251–14256. [CrossRef] [PubMed]
14. Collett, E. *Field Guide to Polarization*, 3rd ed.; SPIE-The International Society for Optical Engineering: Bellingham, WA, USA, 2005; pp. 57–62.
15. Kogelnik, H.; Li, T. Laser beams and resonators. *Appl. Opt.* **1996**, *5*, 1550–1567. [CrossRef] [PubMed]
16. Chen, J.-H.; Chang, R.-S.; Han, C.-Y. Generating a cylindrical vector beam interferometrically for ellipsometric measurement. *Opt. Commun.* **2016**, *361*, 116–123. [CrossRef]